Scientia Horticulturae 212 (2016) 136–147

Contents lists available at ScienceDirect

Scientia Horticulturae

journal homepage: www.elsevier.com/locate/scihorti

Passive reflectance sensing and digital image analysis for assessing quality parameters of mango fruits

Salah Elsayed[a,*], Hoda Galal[a], Aida Allam[a], Urs Schmidhalter[b]

[a] Department of Evaluation and Natural Resources, Environmental Studies and Research Institute, Sadat City University, Egypt
[b] Department of Plant Sciences, Technische Universität München, Emil-Ramann-Str. 2, D-85350 Freising, Germany

ARTICLE INFO

Article history:
Received 7 June 2016
Received in revised form
22 September 2016
Accepted 29 September 2016

Keywords:
Biology
Digital image
Mango
Phenomics
Precision agriculture

ABSTRACT

Actual methods for assessing mango fruit quality are generally based on biochemical analysis, which leads to the destruction of fruits and is time consuming. Similarly, for valuating large quantities of mango fruits for export, numerous observations are required to characterize them; such methods cannot easily account for rapid changes in these parameters. The aims of this study to test the performance of hyperspectral passive reflectance sensing and digital image analysis was tested at various ripening degrees of mango fruits to assess their relationship to biochemical parameters (chlorophyll meter readings, chlorophyll *a*, chlorophyll *b*, total chlorophyll *t*, carotenoids, soluble solids content and titratable acidity) via simple linear regression and partial least square regression (PLSR) analysis. Models of PLSR included (i) spectral reflectance information from 500 to 900 nm, (ii) selected spectral indices, (iii) selected RGB indices from digital image analysis, and (iv) the combination of spectral reflectance indices and RGB indices information. The results showed that the newly developed index (NDVI-VARI)/(NDVI-VARI) showed close and highly significant associations with chlorophyll meter readings, chlorophyll *a* and chlorophyll *t*, with $R^2 = 0.78$, 0.71, and 0.71, respectively, while the normalized difference vegetation index (Red − Blue)/(Red + Blue) was highly significantly related to chlorophyll *b*, carotenoids, soluble solids content and titratable acidity, with R^2 values of 0.57, 0.53, 0.57, and 0.59, respectively. Calibration and validation models of the PLSR analysis based on the combination of data from six spectral reflectance indices and six RGB indices from digital image analysis further improved the relationships to chlorophyll meter readings ($R^2 = 0.91$ and 0.88), chlorophyll *a* ($R^2 = 0.80$ and 0.75), chlorophyll *b* ($R^2 = 0.66$ and 0.57) and chlorophyll *t* ($R^2 = 0.81$ and 0.80), while calibration and validation models of PLSR based on the data from the spectral reflectance range from 500 to 900 nm were most closely related to soluble solids content ($R^2 = 0.72$ and 0.48) and titratable acidity ($R^2 = 0.64$ and 0.49). In conclusion, the assessment of biochemical parameters in mango fruits was improved and more robust when using the multivariate analysis of PLSR models than with previously assayed normalized difference spectral indices and RGB indices from digital image analysis.

1. Introduction

Productive postharvest management and harvest time of mangos demand knowledge of the postharvest physiology or biochemical quality parameters to determine the best handling practices to maintain and create high fruit quality during the ripening stage. Ripening is actually part of the natural senescence regarding mango fruits. It is an irreversible process that contributes to organelle disruption and changes in chemical constituents, flavor and structure. There are different interesting biochemical parameters, such as chlorophyll *a* (Chl *a*), chlorophyll *b* (Chl *b*), total chlorophyll *t* (Chl t), carotenoids (carot), soluble solids content (SSC) and titratable acidity (T. Acid), which can be used as diagnostic indicators of mango quality. Actual methods for the assessment of mango fruit quality are generally based on biochemical analysis, which leads to destruction of fruits and is time consuming. Fruit analysis is important for detecting mango quality; nevertheless, destructive methods are not appropriate. Similarly, for valuating large quantities of mango fruits for export, numerous observations are required for their characterization; such methods cannot easily account for rapid changes in these parameters arising from changes in environmental conditions.

In contrast, high-throughput passive reflectance sensors using spectral reflectance measurements and digital image analysis have

* Corresponding author.
E-mail address: sayed@wzw.tum.de (S. Elsayed).

http://dx.doi.org/10.1016/j.scienta.2016.09.046
0304-4238/

Table 1
Formula, index abbreviation and references of different spectral indices and RGB indices of digital image analysis used in this study.

Formula	Index abbreviation	References
$(R_{850} - R_{710})/(R_{850} + R_{710})$	HPS[a] 850_710	Datt (1999)
$(R_{780} - R_{570})/(R_{780} + R_{570})$	HPS 780_570	Rutkowski et al. (2008)
$(R_{780} - R_{550})/(R_{780} + R_{550})$	HPS 780_550 or GNDVI	Gutierrez et al. (2010)
$(R_{760} - R_{730})/(R_{760} + R_{730})$	HPS 760_730	Barnes et al. (2000)
$(R_{760} - R_{720})/(R_{760} + R_{720})$	HPS 760_720 or NAI	Rouse et al. (1974)
$(R_{750} - R_{710})/(R_{760} + R_{710})$	HPS 760_710	Zarco-Tejada et al. (2005)
$(R_{686} - R_{620})/(R_{686} + R_{620})$	HPS 686_620	this work
$(R_{570} - R_{540})/(R_{570} + R_{540})$	HPS 570_540	this work
(Green − Red)/(Green + Red − Blue)	VARI	Gitelson et al. (2003)
(Green − VARI)/(Green + VARI + Blue)	VARI1	this work
(VARI1 − VARI)/(VARI1 + VARI)	Norm (VARI, VARI1)	this work
(Red − Green)/(Red + Green)	NDVI	Aynalem et al. (2006)
(Red − Blue)/(Red + Blue)	NDVI1	Kawashima and Nakatani (1998)
(NDVI1 − VARI)/(NDVI1 + VARI)	Norm (NDVI1, VARI)	this work

[a] HPS indicates hyperspectral passive sensing.

the potential to provide more information for making better-informed decisions at the mango scale in real time. Passive sensor systems depend on sunlight as a source of light, which allows hyperspectral information to be obtained in the visible and near-infrared range (Elsayed et al., 2011; Erdle et al., 2011; Mistele et al., 2012; Elsayed et al., 2015a; Nagy et al., 2016).

Some previous studies assessed the quality parameters of fruits by using spectroscopic measurements (Rutkowski et al., 2008; Deng et al., 2010; Moghimi et al., 2010; Jha et al., 2012). Rutkowski et al. (2008) found that the index of anthocyanin (NAI), calculated as $(R_{780} - R_{570})/(R_{780} + R_{570})$, was significantly correlated with the fruit firmness and titratable acidity in 'Golden Delicious' apples. Partial least square regression based on spectral reflectance from 400 to 1000 nm, processed with SNV, median filter and 1st derivative, was used to predict the acidity in kiwi fruits (Moghimi et al., 2010). Jha et al. (2012) applied reflectance spectroscopy to measure SSC and pH in seven mango cultivars. The optimal results were obtained by using PLSR models based on 2nd derivative spectra in the 1600–1799 nm range. The reflectance spectrum at 988 nm was significantly correlated with the soluble solids content and vitamin C content of oranges (Deng et al., 2010).

The application of digital cameras and image processing techniques is less expensive than the use of other techniques, such as passive and active reflectance sensing and technologies of satellite imagery. A color camera output can be de-coded into three images to represent the red, green and blue (RGB) components of the full image. The three components of the color image can be recombined using software or hardware to produce intensity, saturation and hue images, which can be more convenient for subsequent processing. Color is considered a fundamental physical property of agricultural products and foods (Ismail and Razali, 2012). The application of digital cameras by using color images has been proven to be a potential source for estimating several fruit quality parameters because the loss of green color is an obvious sign of fruit ripening in many mango cultivars. The development of the optimum skin color usually defines mango quality. Some mango cultivars retain a green color after ripening. Depending on the cultivar, the skin color can change from dark to olive green; sometimes reddish, orange-yellow or yellowish hues appear from the base color. Changes in eight mango selections during ripening included reductions in fruit weight, volume, length, thickness, firmness, pulp content, pulp:peel ratio, starch, and vitamin C and increases in TSS, pH, total sugars, sugar:acid ratio and carotenoid content (Gowda and Huddar, 2000). RGB-based image analysis has been applied in agriculture to detect the chlorophyll and carotenoids of orange fruits (Fouda et al., 2013), sugar content and pH of mangoes (Kondo et al., 2000), total soluble solids, total carbohydrates, titratable acidity and firmness of mango fruits (Domingo et al., 2012), chlorophyll contents of lettuce, broccoli, and tomatoes (Ali et al., 2012), nitrogen status of pepper plants (Yuzhu et al., 2011), and seed color for the identification of commercial seed traits (Dana and Ivo, 2008) and for the estimation of the chlorophyll content in micro propagated plants (Yadav et al., 2010; Dutta Gupta et al., 2013).

For example, applied to relatively few samples of oranges, the R/G band, averages of RGB and the Visible Atmospheric Resistant Index, VARI, showed a sensitive band ratio to different orange properties, such as chlorophyll and carotenoids (Fouda et al., 2013). The average values of red, green and blue of mango fruits under different levels of skin color from green to yellow were correlated with total soluble solids, total carbohydrates, titratable acidity and firmness (Domingo et al., 2012).

The scientific hypothesis raised in this study investigates whether changes in biochemical quality parameters can be reflected by changes in spectral reflectance measurements and digital images analysis based on the change in skin color of mango fruits from dark green to light green. Previous studies have been conducted to evaluate biochemical parameters using PLSR based on spectral reflectance from different bands, but only very few were focused on mango fruits. This study therefore evaluates different models of PLSR based on the full spectral reflectance range, spectral indices, RGB indices of digital image analysis and data combinations from spectral indices and RGB indices to predict biochemical parameters of mango fruits from dark green to light green.

The purpose of this work is to compare the performance of passive reflectance sensing and digital image sensing to assess whether spectral reflectance indices and indices of digital image analysis can reflect the change in biochemical parameters of mango fruits from dark green to light green and to compare the performance of four models of PLSR based on (i) the spectral reflectance from 500 to 900 nm, (ii) the six spectral indices HPS850_710, HPS760_730, HPS760_720, HPS750_710, HPS 686_620 and HPS 570_540 (Table 1), and (iii) six RGB indices of images analysis, namely, the VARI, VARI1, Norm (VARI, VARI1), Norm (NDVI1, VARI), NDVI and NDVI1 (Table 1), as well as (iv) the combination of data from six spectral reflectance indices and six RBG indices, to assess the quality parameters of mangoes.

2. Material and methods

2.1. Experimental information

The experiments were conducted at the Research Station of Sadat City University in Egypt (Latitude: N 30° 2′ 41.185″, Longitude: E 31° 14′ 8.1625″). Mango fruits of the Zabdia cultivar were taken from farms of the research station of Sadat City University. The fruit samples of the mango cultivar were selected at different

ripening degrees to be assessed via passive reflectance and digital image sensing and thereafter used for determining chlorophyll meter readings, chlorophyll *a*, chlorophyll *b*, total chlorophyll *t*, carotenoids, soluble solids content and titratable acidity.

2.2. Biochemical parameters

2.2.1. Total chlorophylls, carotenoids and chlorophyll meter reading (SPAD values)

Total chlorophylls, chlorophyll *a*, chlorophyll *b*, chlorophyll *t* and carotenoids of fruit peel were estimated using the spectrophotometric method recommended by Wettestein (1957) as described by Marković et al. (2012). The spectrophotometer has bands from 390 to 900 nm, and absorptions for the prepared extracts were read at wavelengths of 662, 644 and 440 nm. The quantity of chlorophyll and carotenoids (mg L^{-1}) was calculated according to the following equations and then converted to (μg cm^{-2}).

$$\text{Chl}a(\text{mg L}^{-1}) = 9.784\,A_{662} - 0.990\,A_{644}$$

$$\text{Chl}b(\text{mg L}^{-1}) = 21.426\,A_{644} - 4.650\,A_{662}$$

$$\text{Chl}t(\text{mg L}^{-1}) = \text{Chl}a + \text{Chl}b$$

$$\text{Carotenoids}(\text{mg L}^{-1}) = 4.695\,A_{440} - 0.268(\text{Chl}a + \text{Chl}b)$$

The relative chlorophyll content (SPAD values) was measured by using a portable chlorophyll meter SPAD-502 (Konica-Minolta, Osaka, Japan).

2.2.2. Soluble solids content percentage and titratable acidity

Pulp samples were squeezed and the obtained juice was used to determine the percentage of SSC using a hand refractometer according to AOAC (1980). The titratable acidity was determined in 5 mL of juice samples. For the titration, 0.1 N sodium hydroxide and phenolphthalein as an indicator were used according to AOAC (1980).

2.3. Spectral reflectance measurements

A passive bi-directional reflectance sensor (tec5, Oberursel, Germany), measuring at wavelengths between 302 and 1148 nm with a bandwidth of 2 nm, was used. The handheld FieldSpec sensor consists of two units: one unit is linked with a diffuser and measures the light radiation as a reference signal, while the second unit measures the mango fruits reflectance with a fiber optic (Elsayed et al., 2015b). The aperture of the optics was 12° and the field of view was 0.1 m^2 from half meter distance. Five spectral measurements were taken for each fruit. Spectral measurements of thirty-nine mango fruits under different ripening degrees were taken within 25 min on a sunny period to avoid changes in sun radiation, and the fiber optics were positioned at a height of 0.15 m with a zenith angle of 30° above the mango fruits to avoid producing a shadow. To guarantee complete reflectance by the mango fruits, a black sheet was used to prevent spectral reflectance caused by the background. With the readings from the spectrometer unit, the mango fruitsí reflectance was calculated and corrected with a calibration factor obtained from a reference gray standard.

2.4. Digital image analysis

Mango fruits were photographed by using a Kodak D5100 reflex camera with a 14-megapixel resolution. The camera was manually held and oriented vertically downwards toward the mango fruits at a distance of 50 cm under cloudy conditions to avoid shadows. The digital images were converted from JPEG to PPM file format

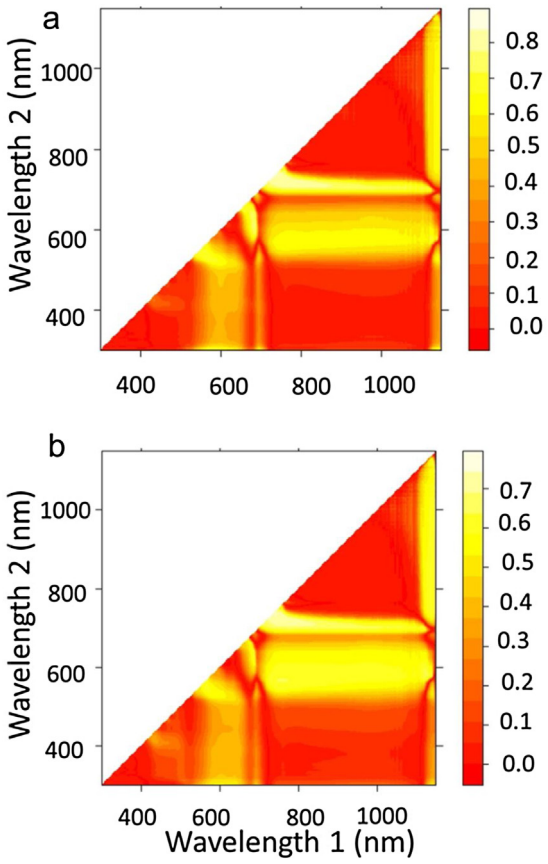

Fig. 1. Correlation matrices (contour maps) showing the coefficients of determination (R^2) for all dual wavelengths combinations in the range of 302–1148 nm (as a normalized difference index) of the hyperspectral passive reflectance sensor with (a) SPAD value and (b) chlorophyll *a* of mango fruits at different ripening degrees.

using IrfanView 4.37. R statistics 3.0.2 (R foundation for Statistical Computing 2013) with the R package "pixmap" was used to calculate six RGB indices from digital image analysis according to the pixels red (R), green (G), and blue (B). The Visible Atmospheric Resistant Index (VARI), a newly developed index of the modified Visible Atmospheric Resistant Index1 (VARI1), a new index of the normalized difference between VARI1 and VARI, the Normalized Difference Vegetation Index (NDVI), the Normalized Difference Vegetation Index1 (NDVI1) and a new index of the normalized difference between NDVI and VARI were tested (Table 1).

2.5. Statistical analysis

2.5.1. Selection of spectral reflectance indices

In Table 1 eight spectral indices from different sources are listed with references. In this study, both known and novel indices were calculated and tested. A contour map analysis for all wavelengths of the hyperspectral passive sensor (from 302 to1048 nm) was used to select some normalized difference indices, which generally presented more stable and strong relationships with the relative chlorophyll content, chlorophyll *a*, chlorophyll *b*, chlorophyll *t*, carotenoids, soluble solids content and titratable acidity of mango fruits. All possible dual wavelengths combinations were evaluated based on a contour map analysis for the hyperspectral passive sensor. Contour maps are matrices of the coefficients of determination of all biochemical parameters of mango fruits with all possible combinations of binary, normalized spectral indices (Fig. 1). The R package "lattice" from the software R statistics version 3.0.2 (R foundation for statistical computing 2013) was used to produce the

Table 2
Minimum, maximum and mean values of seven parameters (SPAD value, chlorophyll *a* (Chl *a*), chlorophyll *b* (Chl *b*), chlorophyll t (Chl t), carotenoids (carot), soluble solids content (SSC) and titratable acidity (T. Acid)) of mango fruits and eight spectral reflectance indices, as well as six RGB indices from digital image analysis.

Parameters			
	Minimum	Maximum	Mean
SPAD value	12.4	36.9	22.4
Chl *a* ($\mu g\,cm^{-2}$)	0.71	3.77	1.88
Chl *b* ($\mu g\,cm^{-2}$)	0.26	1.91	0.91
Chl t ($\mu g\,cm^{-2}$)	1.13	5.14	2.79
Carot ($\mu g\,cm^{-2}$)	0.99	2.79	1.77
SSC (%)	7.10	15.00	10.57
T. Acid. (%)	0.32	1.90	1.25
HPS[1] 850_710	0.032	0.342	0.195
HPS[1] 780_570	0.298	0.681	0.513
HPS 780_550	0.328	0.638	0.501
HPS 760_730	0.004	0.094	0.044
HPS 760_720	0.019	0.206	0.106
HPS 750_710	0.001	0.037	0.018
HPS 686_620	−0.134	0.052	−0.060
HPS 570_540	0.032	0.342	0.195
VARI	−0.10	0.21	0.06
VARI1	0.25	1.25	0.58
Norm (VARI, VARI1)	0.09	1.18	0.74
NDVI	−0.14	0.09	−0.05
NDVI1	0.13	0.65	0.37
Norm (NDVI1, VARI)	−0.23	1.39	0.67

contour maps from the hyperspectral reflectance readings, while twelve wavelengths (810, 780, 760,750, 730, 720, 710, 686, 620, 570, 550 and 540 nm) were used to calculate reflectance indices, as indicated in Table 1.

2.5.2. Modeling of measurements

Sigmaplot for Windows v.12 (Systat software Inc., Chicago) and SPSS 22 (SPSS Inc., Chicago, IL, USA) were used for the statistical analysis. Simple linear regressions were calculated to analyze the relationship between the spectral reflectance indices and RGB indices of digital images analysis listed in Table 1 and the biochemical parameters (Table 2), as well as between the spectral reflectance and RGB indices. Coefficients of determination and significance levels were determined; the nominal alpha value and 0.001 were used (Tables 4, 5, 6). Correlation coefficients analysis between the biochemical parameters in Table 3 and significance levels was determined; nominal alpha values of 0.05 and 0.01 were used.

The Unscrambler X multivariate data analysis software version 10.2 (CAMO Software AS, Oslo) was used to calibrate and validate the partial least square models. Partial Least Square Regression (PLSR) creates orthogonal latent variables across the input variables and relates them to the variables measurements. This is a way to cope with redundancy among the input variables. In this study, the PLSR searches for the sensitive information from spectral reflectance, spectral indices and RGB indices of the digital image analysis. Four models of PLSR based on (i) the spectral reflectance from 500 to 900 nm, (ii) six spectral indices HPS850_710, HPS760_730, HPS760_720, HPS750_710, HPS686_620 and HPS570_540, (iii) six RBG indices of the image analysis, VARI, VARI1, Norm (VARI, VARI1), NDVI, NDVI1 and Norm (NDVI1, VARI), and (iv) the combination of six spectral reflectance indices and six RBG indices for the measured parameters were used as input variables in the PLSR models, as shown in Table 7, for the model datasets of mango fruits at different ripening degrees. In Table 7, a cross validation approach was applied for the PLSR models. Calibration and validation quality of the models are presented through adjusted coefficients of determination of calibration (R^2 cal) and validation (R^2 val) and root mean square errors for calibration (RMSEC) and for validation (RMSEV), and the slopes of the linear regressions between observed and predicted values of all parameters from the calibration and validation models with observed data are shown in Table 7.

3. Results

3.1. Variation of biochemical parameters, spectral reflectance indices and RGB indices from digital image analysis of mango fruits

The results display a wide range between the minimum and maximum values for all biochemical parameters, eight spectral reflectance indices and six RGB indices of the digital image analysis (Table 2). For example, the SPAD values ranged from 12.4 to 36.9, chlorophyll *a* from 0.71 to 3.8 ($\mu g\,cm^{-2}$), chlorophyll *b* from 0.26 to 1.9 ($\mu g\,cm^{-2}$), carotenoids from 0.99 to 2.8 ($\mu g\,cm^{-2}$), the spectral index HPS 780_570 from 0.298 to 0.681, HPS 760_730 from 0.004 to 0.094, HPS 760_720 from 0.019 to 0.206, the VARI1 index from 0.25 to 1.25, and NDVI1 from 0.13 to 0.65. Biochemical parameters, spectral reflectance indices and digital image indices were generally affected by fruit ripening degrees.

3.2. Correlation analysis between the biochemical parameters

In Table 3, correlation analysis indicated that the SPAD value, chlorophyll *a*, chlorophyll *b*, chlorophyll *t*, carotenoids, soluble solids content and titratable acidity were significantly correlated. The highest coefficient of correlation (r) for the biochemical parameters was found for chlorophyll *a* and chlorophyll *t* (r = 0.98**). Statistically significant correlations between all biochemical parameters varied from −0.43** to 0.98**. There were positive correlations between the SPAD value and chlorophyll parameters, while there were negative correlations between the SPAD value, titratable acidity and chlorophyll parameters with carotenoids and the soluble solids content of mango fruits.

Table 3
Correlation coefficients between seven parameters (SPAD value, chlorophyll *a* (Chl *a*), chlorophyll *b* (Chl *b*), chlorophyll t (Chl t), carotenoids (carot), soluble solids content (SSC) and titratable acidity (T. Acid)) of mango fruits.

	SPAD value	Chl *a* ($\mu g\,cm^{-2}$)	Chl *b* ($\mu g\,cm^{-2}$)	Chl t ($\mu g\,cm^{-2}$)	carot ($\mu g\,cm^{-2}$)	SSC (%)	T. Acid. (%)
SPAD value							
Chl *a* ($\mu g\,cm^{-2}$)	0.82**						
Chl *b* ($\mu g\,cm^{-2}$)	0.78**	0.84**					
Chl t ($\mu g\,cm^{-2}$)	0.84**	0.98**	0.93**				
Carot ($\mu g\,cm^{-2}$)	−0.70**	−0.046**	−0.52**	−0.49**			
SSC (%)	−0.68**	−0.50**	−0.45**	−0.50**	0.53**		
T. Acid (%)	0.69**	0.52**	0.54**	0.55**	−0.056**	−0.43**	

** Correlation is significant at the 0.01 level.

Table 4
Coefficients of determination of linear regressions of seven parameters (SPAD value, chlorophyll *a* (Chl *a*), chlorophyll *b* (Chl *b*), chlorophyll t (Chl t), carotenoids (carot), soluble solids content (SSC) and titratable acidity (T. Acid)) with eight spectral indices of the hyperspectral passive sensor (HPS) (calculated as normalized difference indices) of mangoes.

Spectral indices	SPAD value	Chl *a* ($\mu g\,cm^{-2}$)	Chl *b* ($\mu g\,cm^{-2}$)	Chl t ($\mu g\,cm^{-2}$)	carot ($\mu g\,cm^{-2}$)	SSC (%)	T. Acid (%)
HPS[1] 850_710	0.79***	0.74***	0.57***	0.73***	0.33***	0.50***	0.46***
HPS 780_570	0.66***	0.66***	0.53***	0.66***	0.22**	0.45***	0.38***
HPS 780_550	0.60***	0.62***	0.47***	0.61***	0.16*	0.42***	0.33***
HPS 760_730	0.83***	0.79***	0.59***	0.77***	0.32***	0.54***	0.48***
HPS 760_720	0.83***	0.79***	0.60***	0.78***	0.33***	0.52***	0.49***
HPS 760_710	0.81***	0.79***	0.59***	0.77***	0.30***	0.50***	0.47***
HPS 686_620	0.78***	0.62***	0.53***	0.65***	0.40***	0.57***	0.39***
HPS 570_540	0.77***	0.67***	0.60***	0.69***	0.48***	0.50***	0.50***

* Statistically significant at $P \leq 0.05$.
** Statistically significant at $P \leq 0.01$.
*** Statistically significant at $P \leq 0.001$.

Table 5
Coefficients of determination of linear regressions of the seven parameters (SPAD value, chlorophyll *a* (Chl *a*), chlorophyll *b* (Chl *b*), chlorophyll t (Chl t), carotenoids (carot) soluble solids content (SSC) and titratable acidity (T. Acid)) with six RGB indices from digital image analysis.

Indices	SPAD value	Chl *a* ($\mu g\,cm^{-2}$)	Chl *b* ($\mu g\,cm^{-2}$)	Chl t ($\mu g\,cm^{-2}$)	carot ($\mu g\,cm^{-2}$)	SCC (%)	T. Acid (%)
VARI	0.73***	0.66***	0.51***	0.66***	0.38***	0.40***	0.38***
VARI1	0.68***	0.64***	0.52***	0.64***	0.44***	0.46***	0.47***
Norm (VARI,VARI)	0.75***	0.67***	0.51***	0.66***	0.35***	0.38***	0.36***
NDVI	0.68***	0.63***	0.49***	0.62***	0.38***	0.38***	0.36***
NDVI1	0.77***	0.67***	0.57***	0.68***	0.53***	0.57***	0.59***
Norm (NDVI1, VARI)	0.78***	0.71***	0.56***	0.71***	0.37***	0.41***	0.42***

*** Statistically significant at $P \leq 0.001$, respectively.

3.3. Contour map analysis of the hyperspectral data

A contour map analysis produced the coefficients of determination (R^2) of the measurements for all dual wavelengths combinations from 302 to 1148 nm as a normalized difference spectral index. Contours of the matrices of the hyperspectral passive sensor presented generally more distinct relationships with all biochemical parameters. The contour map analysis of the relationship between the normalized difference spectral indices with the SPAD value and chlorophyll *a* is shown in Fig. 1.

3.4. Relationships between spectral reflectance indices and different biochemical parameters

In Table 4 & Fig. 2, nine spectral reflectance indices were significantly related to all biochemical parameters. Statistically significant relationships between all spectral reflectance indices derived from the visible VIS, near infrared NIR or the combination of VIS and NIR regions were found for the SPAD value with R^2 values ranging from 0.66*** to 0.83***, chlorophyll *a* with R^2 values ranging from 0.62*** to 0.79***, chlorophyll *b* with R^2 values ranging from 0.47*** to 0.60***, chlorophyll *t* with R^2 values ranging from 0.61** to 0.78***, carotenoids with R^2 values ranging from 0.16* to 0.48***, soluble solids content with R^2 values ranging from 0.42*** to 0.57*** and titratable acidity with R^2 values ranging from 0.33*** to 0.50***. Generally, the normalized spectral indices HPS 760_730, 760_720 and 686_620 showed the highest coefficients of determination for the SPAD value, chlorophyll *a*, chlorophyll *b* and chlorophyll *t* of mango fruits.

3.5. Relationships between six RGB indices from digital image analysis and biochemical parameters

The six RGB indices from digital image analysis were related to the biochemical parameters (Table 5 & Fig. 3). The highest coefficients of determination (R^2) were found for the index (NDVI1 − VARI)/(NDVI1 + VARI) and the SPAD value ($R^2 = 0.78$***). Statistically significant relationships between the six RGB indices obtained from digital image analysis and all biochemical parameters varied from 0.36*** to 0.78***.

3.6. Relationships between six RGB indices from digital image analysis and eight spectral indices

The relationships between six RGB indices from digital image analysis and eight spectral indices varied from 0.48*** to 0.74***, as shown in Table 6. The highest coefficient of relationship (R^2) was found between the index VARI1 derived from image analysis and the spectral index HPS 570_540 ($R^2 = 0.78$***).

3.7. Partial least squares regression analysis to predict the measured parameters

In Table 7 (Figs. 4 and 5), the quality of the four PLSR models is presented through adjusted coefficients of determination of calibration (R^2 cal) and validation (R^2 val), the root mean square errors (RMSE cal and val), and the slope of the linear regressions for the calibration and validation models. Across all calibration dataset formations, the coefficients of determination of model (i) varied from 0.57*** to 0.91***, of model (ii) from 0.57*** to 0.87***, of model (iii) from 0.56*** to 0.82*** and of model (iv) from 0.62*** to 91*** for all biochemical parameters. Across all validation data set formations, the coefficients of determination for model (i) varied from 0.48*** to 0.86***, for model (ii), from 0.48*** to 0.85***, for model (iii), from 0.49*** to 0.80*** and for model (iv), from 0.52*** to 88*** for all biochemical parameters. For example, across all calibration and validation data set formations of model (i), the RMSE varied from 2.27 to 3.53 for the SPAD value, from 0.33 to 0.40 ($\mu g\,cm^{-2}$) for chlorophyll *a*, from 0.21 to 0.27 ($\mu g\,cm^{-2}$) for chlorophyll *b* and from 0.46 to 0.62 ($\mu g\,cm^{-2}$) for chlorophyll *t*. The highest slopes for calibration and validation data sets for all models were 0.91 and 0.90, respectively, for the SPAD value obtained using model (iv).

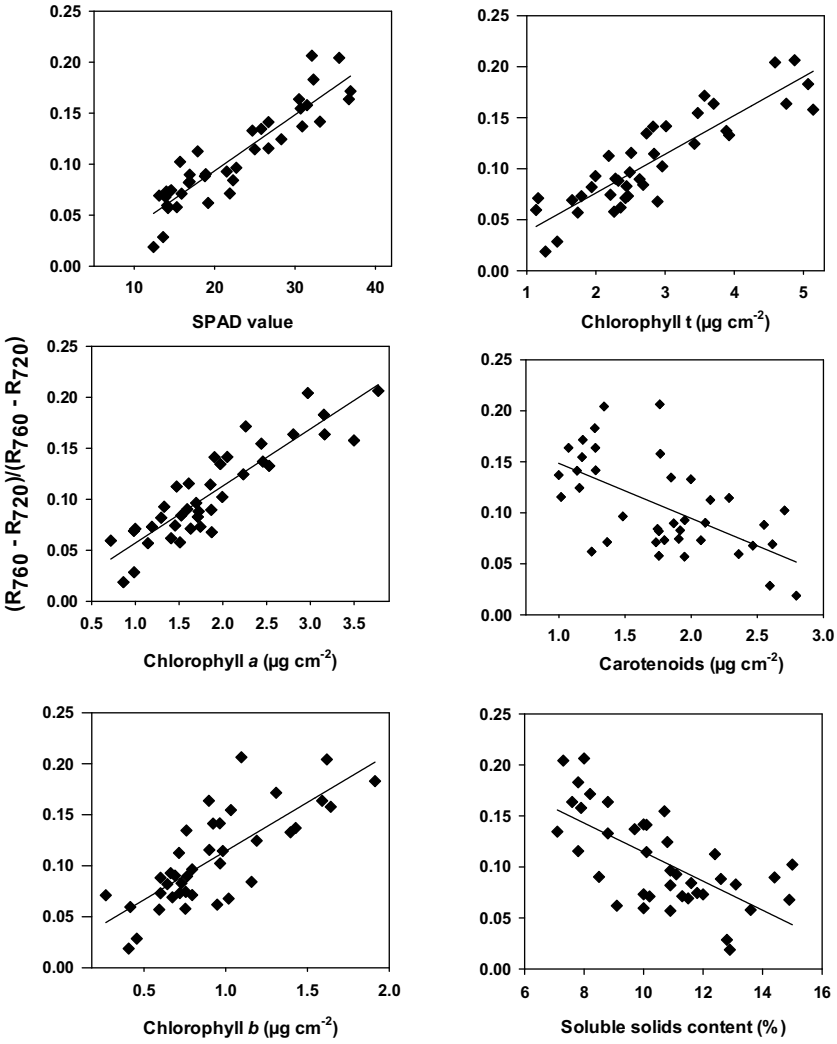

Fig. 2. The relationship between the spectral index HPS 760_720 and the SPAD value, chlorophyll *a*, chlorophyll *b*, chlorophyll t, carotenoids and soluble solids content of mango fruits. Statistical information is given in Table 4.

Table 6
Coefficients of determination of linear regressions of the six RBG indices of digital image analysis and eight spectral indices of the hyperspectral passive sensor (HPS) (calculated as normalized difference indices) of mango fruits.

Indices	HPS 850_710	HPS 760_730	HPS 760_720	HPS 750_710	HPS 686_620	HPS 570_540	HPS 780_570	HPS 780_550
VARI	0.63***	0.66***	0.69***	0.68***	0.64***	0.70***	0.57***	0.50***
VARI1	0.64***	0.64***	0.66***	0.64***	0.62***	0.74***	0.59***	0.51***
Norm (VARI,VARI)	0.61***	0.67***	0.70***	0.67***	0.63***	0.65***	0.54***	0.48***
NDVI	0.61***	0.63***	0.66***	0.64***	0.63***	0.71***	0.56***	0.49***
NDVI1	0.68***	0.70***	0.70***	0.69***	0.60***	0.68***	0.57***	0.51***
Norm (NDVI1, VARI)	0.66***	0.71***	0.73***	0.71***	0.64***	0.68***	0.58***	0.52***

*** Statistically significant at $P \leq 0.001$, respectively.

4. Discussion

Passive reflectance sensing and digital image analysis were used in this study to assess the chlorophyll meter readings (SPAD values), chlorophyll, carotenoid, soluble solids content and titratable acidity of mango fruits at different ripening degrees. The results showed that during fruit ripening, the values of SPAD, chlorophyll *a*, chlorophyll *b*, chlorophyll *t* and titratable acidity were decreased and the skin color changed from medium green to light green, while the values of carotenoids and soluble solids content were increased and showed negative relationships with the above parameters (Table 3). Significant relationships with all biochemical parameters could be established (Table 3). These results agree with other studies. For example, Medlicott et al. (1986) reported that during fruit ripening, the chlorophyll concentration decreased substantially, whereas the carotenoid concentration increased. Color changes in mango fruit are due to the disappearance of chlorophyll and the appearance of other pigments. Chloroplasts are transformed into chloroplasts containing yellow or red pigments (Lizada, 1993). The soluble solids content also increases during ripening because starch and sucrose are converted into glucose, which is the main substrate utilized in respiration (Chan and Kwok, 1975).

Our assessment of reflectance indices as a method to assess the chlorophyll meter readings (SPAD values), chlorophyll, carotenoids, soluble solids content and titratable acidity of mango fruits at different ripening degrees demonstrated that the selected

Table 7
Calibration (R^2 cal, RMSEC and slope cal) and validation (R^2 val, RMSEV and slope val) of the statistics of four partial least square regression models of (i) the spectral reflectance from 500 to 900 nm, (ii) six spectral indices: HPS850_710, HPS760_730, HPS760_720, HPS750_710, HPS686_620 and HPS570_540, (iii) six RBG indices: VARI, VARI1, Norm (VARI, VARI1), NDVI, NDVI1 and Norm (NDVI1, VARI), and (iv) the combined data of six spectral indices and RBG indices for the SPAD value, chlorophyll *a* (Chl *a*), chlorophyll *b* (Chl *b*), chlorophyll t (Chl t), carotenoids (carot), soluble solids content (SSC) and titratable acidity (T. Acid) of mango fruits.

Models	Statistical parameters	[1]PCs	SPAD value	PCs	Chl *a* ($\mu g\,cm^{-2}$)	PCs	Chl *b* ($\mu g\,cm^{-2}$)	PCs	Chl t ($\mu g\,cm^{-2}$)	PCs	carot ($\mu g\,cm^{-2}$)	PCs	SSC (%)	PCs	T. Acid (%)
Spectral reflectance (500–900 nm)	R^2 cal	5	0.91***	4	0.77***	3	0.57***	5	0.79***	4	0.61***	7	0.72***	6	0.64***
	R^2 val		0.86***		0.70***		0.48***		0.69***		0.51***		0.48***		0.49***
	RMSEC		2.27		0.34		0.24		0.48		0.35		1.22		0.26
	RMSEV		2.91		0.40		0.27		0.59		0.41		1.75		0.32
	Slope cal		0.91		0.77		0.57		0.79		0.61		0.72		0.64
	Slope val		0.90		0.76		0.52		0.75		0.53		0.68		0.58
Six spectral indices	R^2 cal	2	0.87***	2	0.77***	2	0.62***	3	0.79***	6	0.67***	2	0.57***	2	0.53***
	R^2 val		0.85***		0.75***		0.57***		0.74***		0.55***		0.51***		0.48***
	RMSEC		2.70		0.34		0.22		0.48		0.32		1.51		2.95
	RMSEV		2.97		0.38		0.24		0.55		0.39		1.66		3.18
	Slope cal		0.87		0.77		0.62		0.79		0.68		0.57		0.53
	Slope val		0.85		0.75		0.60		0.78		0.65		0.53		0.5
Six RGB indices from digital image analysis	R^2 cal	3	0.82***	1	0.71***	1	0.56***	1	0.70***	3	0.56***	3	0.58***	3	0.63***
	R^2 val		0.80***		0.68***		0.54***		0.67***		0.49***		0.51***		0.57***
	RMSEC		3.20		0.40		0.24		0.59		0.39		1.46		0.27
	RMSEV		3.53		0.40		0.25		0.62		0.43		1.60		0.29
	Slope cal		0.82		0.71		0.56		0.70		0.56		0.58		0.63
	Slope val		0.82		0.68		0.54		0.68		0.52		0.55		0.58
Six spectral indices with six RGB indices from image analysis	R^2 cal	3	0.91***	2	0.80***	3	0.66***	3	0.81***	5	0.65***	3	0.65***	2	0.62***
	R^2 val		0.88***		0.75***		0.57***		0.80***		0.52***		0.57***		0.56***
	RMSEC		2.35		0.33		0.21		0.46		0.34		1.33		0.27
	RMSEV		2.65		0.38		0.25		0.53		0.42		1.49		0.29
	Slope cal		0.91		0.80		0.66		0.81		0.65		0.65		0.62
	Slope val		0.90		0.76		0.61		0.79		0.60		0.59		0.54

Statistically significant at $P \leq 0.001$; [1]PCs, Number of latent variables; Cal, Calibration; Val, Validation; RMSEC, Root mean square error for calibration; RMSEV, Root mean square error for validation.

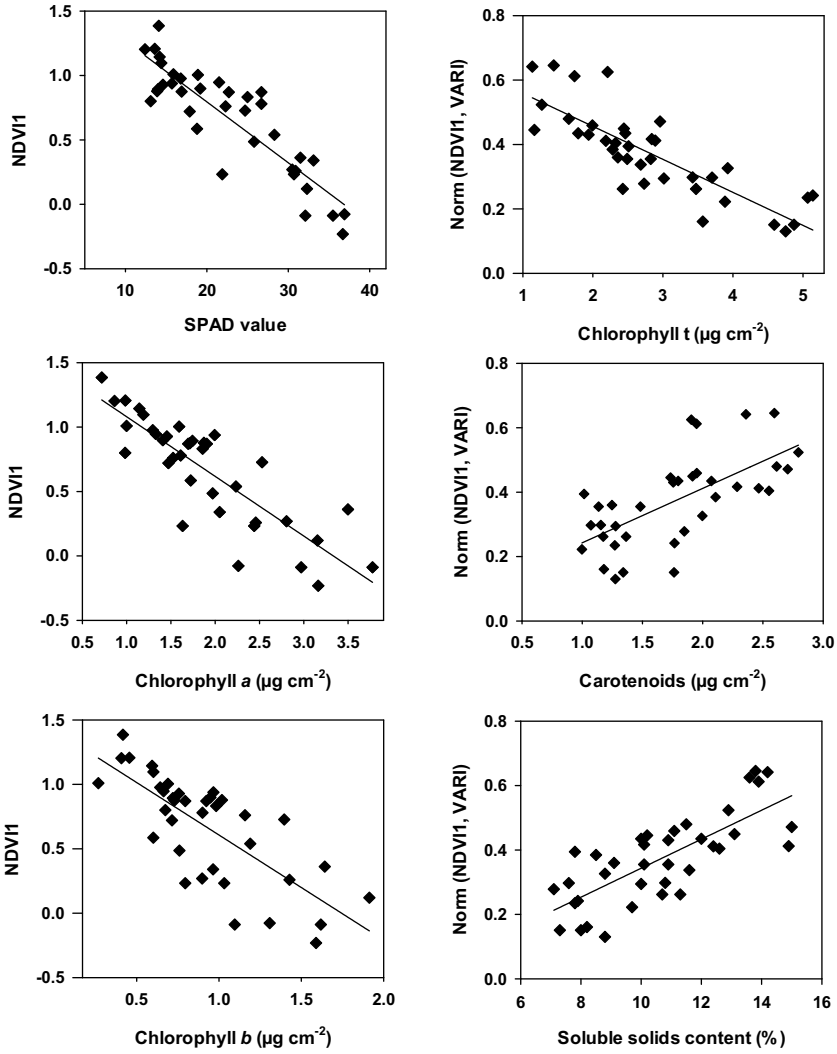

Fig. 3. Relationship between NDV1 and Norm (NDVI1, VARI) of SPAD values, chlorophyll *a*, chlorophyll *b*, chlorophyll t, carotenoids and soluble solids content of mango fruits. Statistical information is given in Table 5.

eight indices, i.e., HPS 850_710, HPS 760_730, HPS 760_720 and HPS 750_710, which were derived from the near infrared region, HPS 686_620 and HPS 570_540, which were derived from the visible region, and HPS 780_570 and HPS 780_550, which were derived from the combinations between the visible and near infrared regions, were apparently useful for describing these parameters (Table 4). All spectral indices showed significant relationships with the measured parameters, and the coefficients of determination varied from 0.16* to 0.83*** for all investigated parameters. Two indices, i.e., HPS 760_730 and HPS 760_720, showed the highest R^2-values with respect to chlorophyll meter readings (0.83*** for both), chlorophyll *a* (0.79*** for both), chlorophyll *b* (0.59*** and 0.60***) and chlorophyll *t* (0.77*** and 0.78***), while HPS 570_540 showed the highest R^2 with respect to carotenoids (0.48***) and titratable acidity (0.50***) and HPS 686_620 showed the highest R^2 with respect to the soluble solids content (0.57***). The indices with better relationships with the chlorophyll parameters were based on the red edge or the near infrared bands.

Some studies have reported that different biochemical parameters can be assessed remotely and estimated simultaneously in a rapid and nondestructive method if these parameters present a significant relationship with the spectral reflectance indices (Merzlyak et al., 2003; Zude et al., 2006; Rutkowski et al., 2008; Deng et al., 2010). For example, Zude et al. (2006) found relations between the peak absorbance of chlorophyll *a* at 680 nm and the soluble solids content (R^2 = 0.21) in apple fruits. Rutkowski et al. (2008) found that the index of anthocyanin (NAI), calculated as $(R_{780} - R_{570})/(R_{780} + R_{570})$, was significantly related to titratable acid (R^2 = 0.66) in 'Golden Delicious' apples. Deng et al. (2010) found that the reflectance spectrum at 988 nm was significantly related to the soluble solids content (R^2 = 0.15) in orange fruits. Merzlyak et al. (2003) found that the reflectance ratios R_{800}/R_{700} and R_{800}/R_{640} were directly proportional to the total chlorophyll content, ranging from 0.4 to 11 nmol cm^{-2}, in apple fruits. The reflectance in the 520–530 nm band was found to be dependent mostly on carotenoids absorption. The index R_{800} $(1/R_{520} - 1/R_{700})$ was suggested for the estimation of the carotenoid content in the range of 0.6–4.5 nmol cm^{-2}. Our results for spectral reflectance indices presented stronger relationships with the biochemical parameters of mango fruits compared to the above indices.

The RGB indices of the image analysis were used in this study because the color of fruits has been found to correlate well with other physical, chemical and sensorial indicators of product quality. The surface color of a fruit is a major visual parameter that has been used traditionally to determine its ripeness. The change in color during fruit ripening is due to the unmasking of previously present pigments due to the degradation of chlorophyll (Tucker and Grierson, 1987; Lizada, 1993).

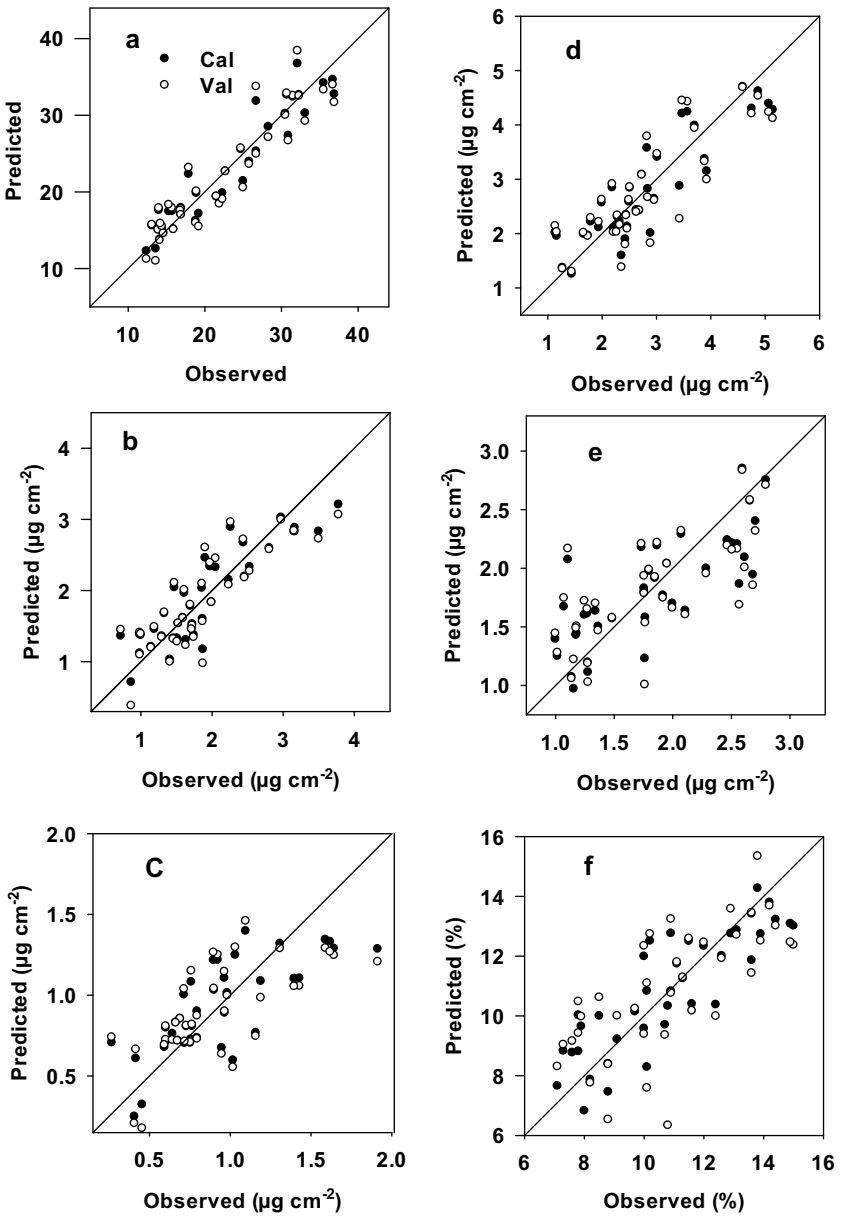

Fig. 4. Relationships between observed and predicted (a) SPAD values, (b) chlorophyll *a*, (c) chlorophyll *b*, (d) chlorophyll t, (e) carotenoids and (f) soluble solid contents of mango fruits for the calibration and validation datasets using partial least square regression models. Statistical information is given in Table 7.

The newly developed and the previous six indices from the image analysis (Table 5) showed significant relationships with all biochemical parameters. The new index (NDVI –VARI)/(NDVI – VARI) showed the highest R^2-values with chlorophyll meter readings (0.78***), chlorophyll *a* (0.71***) and chlorophyll *t* (0.71***), while the normalized difference vegetation index (Red – Blue)/(Red + Blue) presented the highest R^2 with chlorophyll *b* (0.57***), carotenoids (0.53***), soluble solids content (0.57***) and titratable acidity (0.59***). All indices from the image analysis presented stronger relationships with chlorophyll meter readings, chlorophyll *a*, chlorophyll *b* and chlorophyll *t* compared to their relationships with carotenoids, soluble solids content and titratable acidity. The indices VARI1 (Green – VARI)/(Green + VARI + Blue), Norm (VARI, VARI1) and (NDVI-VARI)/(NDVI-VARI) presented the closest associations with all biochemical parameters.

With a reduced set of orange cultivars, Fouda et al. (2013) observed quadratic relationships for the VARI and Ratio (Red/Green) band with chlorophyll *a*, chlorophyll *b* and carotenoids, and the saturation effect of these indices became apparent when the value of chlorophyll *a* was higher than 17 mg kg^{-1} and the value of chlorophyll *b* was larger than 25 mg kg^{-1}, as well as when the value of carotenoids was lower than 50 mg kg^{-1}. Our data presented linear relationships between the RGB indices from the image analysis and biochemical parameters. Domingo et al. (2012) depicted relationships between RGB values with firmness and total carbohydrates, while RGB values were not related to the titratable acidity of 'Sinta' Papaya mango fruits. Our data show that significant relationships between the seven RGB indices and the titratable acidity of Zabdia mango fruits exist and that the normalized difference vegetation index (Red – Blue)/(Red + Blue) presents the highest R^2-values of 0.59*** with the titratable acidity. The results showed that the photometric method, using a digital camera, can be used to quantitatively determine the biochemical parameters of mango fruits.

In this study, six RGB indices and eight spectral indices proved to be useful and could be used to replace passive reflectance sensing

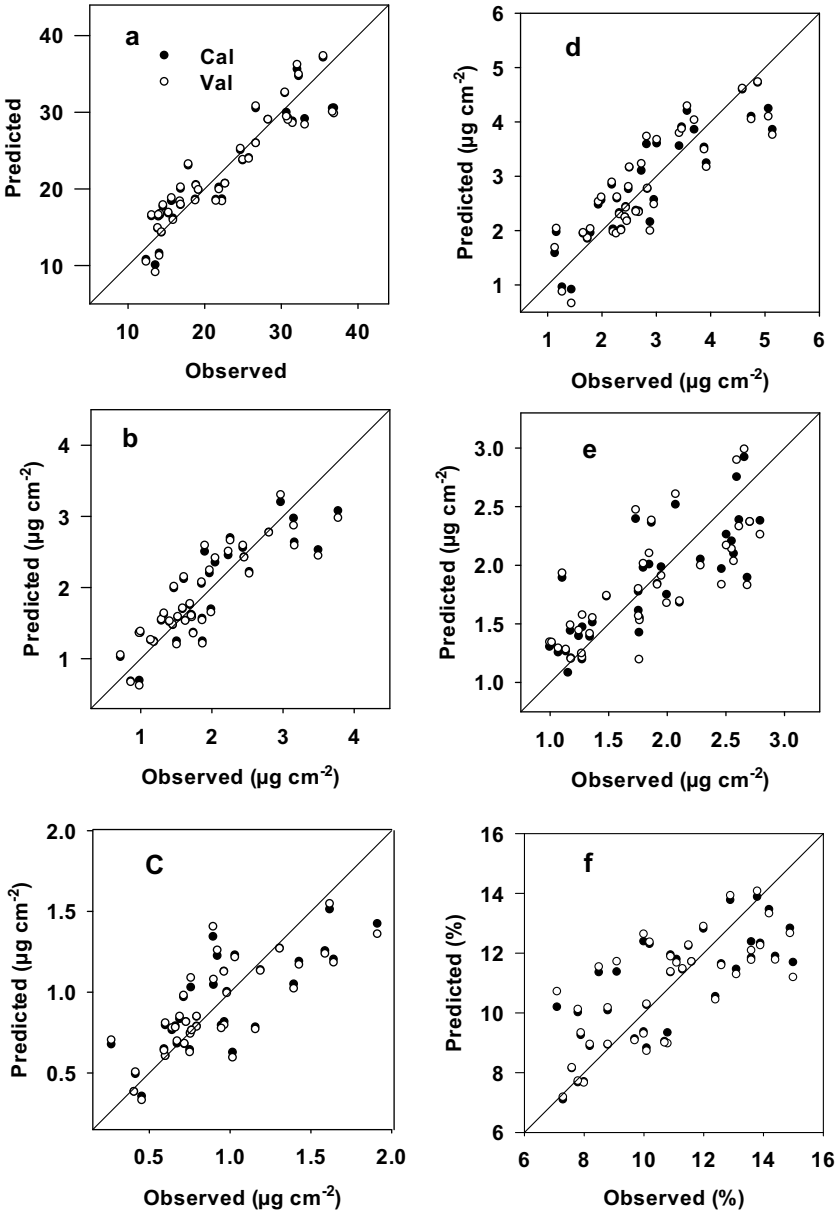

Fig. 5. Relationships between observed and predicted values of (a) SPAD, (b) chlorophyll *a*, (c) chlorophyll *b*, (d) chlorophyll t, (e) carotenoids and (f) soluble solids content of mango fruits for the calibration and validation datasets using a partial least square regression model. Statistical information is given in Table 7.

by using a digital camera. The data showed that strong and significant relationships existed between them. VARI was strongly related to HPS 686_620, VARI1 with HPS 570_540, Norm (VARI, VAR1) with HPS 760_720, NDVI with HPS 570_540, NDVI1 with HPS 760_730 and HPS 760_720, and Norm (NDVI, VARI) with HPS 760_720 (Table 6).

The results from this study show that the four models of partial least square regression obtained from the data of passive reflectance sensing and digital imaging could be used individually or in combination to predict the biochemical parameters. The use of the PLSR analysis increased the accuracy of the estimates of all biochemical parameters (Table 7) compared with the use of the normalized difference spectral indices (Table 4) and the RGB indices from the image analysis (Table 5). The PLSR technique allows for identifying optimized models and is considered as a state-of-the art technique that enables high efficiency when searching for optimized relationships. Simple linear, polynomial or exponential functions are used to model the relationship between the biophysical parameters and the VIs. Alternatively, non-linear regression techniques like Support Vector Regression (SVR) can be applied. The experience further shows that overfitting should be avoided and attention should be paid to the robustness of the tested algorithms. The advantage of the PLSR models compared with normalized spectral indices and RGB indices is that the PLSR in this study used either information from the spectrum from 500 to 900 nm, from eight spectral indices, from six RGB indices, or from eight spectral indices together with six RGB indices and selected the number of factors to best represent the calibration data without overfitting. PLSR had no limitation in predicting the measured parameters, and the relationship between the observed and predicted values was linear (Elsayed et al., 2015a). The calibrations and the validations of the four models of the PLSR analysis were strongly related to the biochemical parameters, compared with the normalized difference spectral indices (Table 4) and the RBG indices from the image analysis (Table 5). The calibration and the validation of the models from PLSR based on the combination of data from six spectral reflectance indices and six RBG image analyses showed

the highest R^2-values with chlorophyll meter readings (0.91*** and 0.88***), chlorophyll *a* (0.80*** and 0.75***), chlorophyll *b* (0.66*** and 0.57***) and chlorophyll *t* (0.81*** and 0.80***). The calibration and the validation models of the PLSR based on the data from the six spectral reflectance indices showed the highest R^2-values with carotenoids (0.67*** and 0.55***). The calibration and the validation models of the PLSR based on the data from the spectral reflectance measurements (500–900 nm) showed the highest R^2 with soluble solids content (0.72*** and 0.48***) and titratable acidity (0.64*** and 0.49***). Comparably, in mango fruits, the assessment of biochemical parameters was stronger and more robust when using PLSR models than with the previously assayed normalized difference spectral indices and RGB indices. This is shown by the improvement of the coefficients of determination in Table 7.

These results agree with previous studies, which only used models of PLSR based on the range of the spectral reflectance to estimate biochemical parameters of different fruits. In contrast, our results showed improved relationships due to data fusion, selecting thus the best models for estimating the biochemical parameters of mango fruits. For example, Paz et al. (2008) applied Vis/NIR reflectance spectra to predict the soluble solids content in plums. The soluble solids content could be predicted using a modified PLSR model based on spectra in the 515–1400 nm range, with R^2 of 0.77 and SECV of 0.83° Brix. Jha et al. (2012) applied reflectance spectroscopy to measure the soluble solids content and pH in seven mango cultivars. The optimal results were obtained by using PLSR models based on the 2nd derivative spectra in the 1600–1799 nm range, with R^2 of 0.57 and 0.49 and SEP of 3.23 and 0.72, respectively. Moghimi et al. (2010) predicted the acidity in kiwi fruits using transmittance spectra in the 400–1000 nm range. A PLSR model based on spectra processed with SNV, median filter and 1st derivative could yield a result with R^2 of 0.88 and RMSEP of 0.076. Fernandez-Novales et al. (2009) estimated tartaric acid using NIR transmittance spectra in the 700–1060 nm wavelength range with less accurate results (R^2 = 0.27, RMSECV = 0.22).

The calibration and validation of models of the PLSR analysis from the combination of six spectral reflectance indices and six RGB image analyses, as well as the spectral reflectance from 500 to 900 nm, generally showed the highest slopes and lowest RMSE of all biochemical parameters compared with the other models.

5. Conclusions

The results show that changes in biochemical parameters of mango fruits at various ripening degrees can reliably be detected using models of partial least squares regression, spectral reflectance indices and RGB indices from image analysis. Models of partial least square regression could further improve the assessment of biochemical parameters of mango fruits compared to spectral indices and RGB indices from image analysis. We have further work to establish active and passive sensor platform based on the best indicators of spectral indices, RGB indices values and the best calibration model of partial least square regression for assessment the fruit ripeness, since the values of these indicators were varied depend on the fruit ripeness.

Acknowledgement

The authors acknowledge the financial support by Sadat City University in Egypt and the International Bureau of the German Federal Ministry of Education and Research (Project No: 01DH12046).

References

AOAC, 1980. Official Methods of Analysis, 13th ed. Association of Official Analytical Chemists, Washington, D.C, USA.
Ali, M.M., Al-Ani, A., Eamus, D., Tan, D.K.Y., 2012. A new image processing based technique to determine chlorophyll in plants. Am. Eurasian J. Agric. Environ. Sci. 12, 1323–1328.
Aynalem, H.M., Righetti, T.L., Reed, B.M., 2006. Non-destructive evaluation of in vitro-stored plants: a comparison of visual and image analysis, in vitro. Cell. Dev. Biol. Plant. 42, 562–567.
Barnes, E.M., Clarke, T.R., Richards, S.E., Colazzi, P.D., Haberland, J., Kostrzewski, M., 2000. Coincident detection of crop water stress, nitrogen status and canopy density using ground-based multispectral data. In: Proceedings of the 5th International Conference on Precision Agriculture, Bloomington, MN, USA.
Chan, H.T., Kwok, S.C.M., 1975. Importance of enzyme inactivation prior to extraction of sugars from papaya. J. Food. Sci. 40, 770–774.
Dana, W., Ivo, W., 2008. Computer image analysis of seed shape and seed color of flax cultivar description. Comput. Electron. Agric. 61, 126–135.
Datt, B., 1999. Visible/near infrared reflectance and chlorophyll content in Eucalyptus leaves. Int. J. Remote Sens. 20, 2741–2759.
Deng, L., He, S., Yi, S., Zheng, Y., Xie, R., Zhang, X., Mao, S., 2010. Study on synchronous correlation between fruit characteristic spectrum and the parameter of internal quality for Hamlin sweet orange fruit. Spectrosc. Spectr. Anal. 30, 1049–1052.
Domingo, L.D., Serrano, P.B., Serrano, P.E., del Rosario, E.J., 2012. Digital photometric method for determining degree of harvest maturity and ripeness of 'Sinta' Papaya (*Carica papaya* L.) fruits. Philipp. Agric. Sci. 3, 252–259.
Dutta Gupta, S., Ibaraki, Y., Pattanayak, A., 2013. Development of a digital image analysis method for real-time estimation of chlorophyll content in micro-propagated potato plants. Plant Biotechnol. Rep. 7, 91–97.
Elsayed, S., Mistele, B., Schmidhalter, U., 2011. Can changes in leaf water potential be assessed spectrally? Funct. Plant Biol. 38, 523–533.
Elsayed, S., Elhoweity, M., Schmidhalter, U., 2015a. Normalized difference spectral indices and partial least squares regression to assess the yield and yield components of peanut. Aust. J. Crop Sci. 9, 976–986.
Elsayed, S., Rischbeck, P., Schmidhalter, U., 2015b. Comparing the performance of active and passive reflectance sensors to assess the normalized relative canopy temperature and grain yield of drought-stressed barley cultivars. Field Crops Res. 177, 148–160.
Erdle, K., Mistele, B., Schmidhalter, U., 2011. Comparison of active and passive spectral sensors in discriminating biomass parameters and nitrogen status in wheat cultivars. Field Crop Res 124, 74–84.
Fernandez-Novales, J., Lopez, M.I., Sanchez, M.T., Garcia-Mesa, J.A., Gonzalez-Caballero, V., 2009. Assessment of quality parameters in grapes during ripening using a miniature fiber-optic near-infrared spectrometer. Int. J. Food Sci. Nutr. 60, 265–277.
Fouda, T., Derbala, A., Elmetwalli, A., Salah, S., 2013. Detection of orange color using imaging analysis. AgroLife Sci. J. 2, 181–184.
Gitelson, A.A., Solovchenko, E.A., Merzlyak, N.M., 2003. Reflectance spectral features and non-destructive estimation of chlorophyll: carotenoid and anthocyanin content in apple fruit. Postharvest Biol. Tecnol. 27, 197–211.
Gowda, I.N.D., Huddar, A.G., 2000. Evaluation of mango hybrids for storage behaviour and sensory qualities. J. Food Sci. Technol. 37, 620–623.
Gutierrez, M., Reynolds, M.P., Raun, W.R., Stone, M.L., Klatt, A.R., 2010. Spectral water indices for assessing yield in elite bread wheat genotypes in well irrigated, water stressed, and high temperature conditions. Crop Sci. 50, 197–214.
Jha, S.N., Jaiswal, P., Narsaiah, K., Gupta, M., Bhardwaj, R., Singh, A.K., 2012. Non-destructive prediction of sweetness of intact mango using near infrared spectroscopy. Sci. Hortic. 138, 171–175.
Kawashima, S., Nakatani, M., 1998. An algorithm for estimating chlorophyll content in leaves using a video camera. Ann. Bot. 81, 49–54.
Kondo, N., Ahmed, U., Monta, M., Murase, H., 2000. Machine vision based quality evaluation of Iyokan orange fruit using neural networks. Comput. Electron. Agric. 29, 135–147.
Lizada, M.C.C., 1993. Mango. In: Seymour, G.B., Taylor, J.E., Tucker, G.A. (Eds.), Biochemistry of Fruit Ripening. Chapman and Hall, London, pp. 257–271.
Marković, M.S., Pavlović, D.V., Tošić, S.M., Stankov-Jovanović, V.P., Krstić, N.S., Stamenković, S.M., Mitrović, T.L.J., Matković, V.L.J., 2012. Chloroplast pigments in post-fire grown cryptophytes on Vidlič Mountain (Southeastern Serbia). Arch. Biol. Sci. 64, 531–538.
Medlicott, A.P., Bhogal, M., Reynolds, S.B., 1986. Changes in peel pigmentation during ripening of mango fruit (*Mangifera indica* var Tommy Atkins). Ann. Appl. Biol. 109, 651–656.
Merzlyak, M., Solovchenko, A., Gitelson, A., 2003. Reflectance spectral features and non-destructive estimation of chlorophyll, carotenoid and anthocyanin content in apple fruit. Postharvest Biol. Tecnol. 27, 197–211.
Mistele, B., Elsayed, S., Schmidhalter, U., 2012. Assessing water status in wheat under field conditions using laser induced chlorophyll fluorescence and hyperspectral measurements. In: 11th International Conference on Precision Agriculture, Indianapolis, Indiana USA.
Moghimi, A., Aghkhani, M.H., Sazgarnia, A., Sarmad, M., 2010. Vis/Nir spectroscopy and chemometrics for the prediction of soluble solids content and acidity (pH) of kiwifruit. Biosyst. Eng. 106, 295–302.
Nagy, A., Riczu, P., Tamás, J., 2016. Spectral evaluation of apple fruit ripening and pigment content alteration. Sci. Hort. 201, 256–264.

Paz, P., Sanchez, M.T., Perez-Marin, D., Guerrero, J.E., Garrido-Varo, A., 2008. Nondestructive determination of total soluble solid content and firmness in plums using near-infrared reflectance spectroscopy. J. Agric. Food Chem. 56, 2565–2570.

Rouse, J.W., Haas, R.H., Schell, J.A., Deering, D.W., Harlan, J.C. 1974. Monitoring the vernal advancement of retro gradation of natural vegetation. NASA/GSFC, Type lll. Final Report. Greenbelt MD, USA.

Rutkowski, K.P., Michalczuk, B., Konopacki, P., 2008. Nondestructive determination of 'golden delicious' apple quality and harvest maturity. J. Fruit Ornam. Plant Res. 16, 39–52.

Tucker, G.A., Grierson, D., 1987. Fruit ripening. In: Davies, D. (Ed.), The Biochemistry of Plants, 12. Academic Press Inc, New York, pp. 265–319.

Wettestein, V.D., 1957. Chlorophyll—lethale und submikroskopische formwechsel der plastiden. Exp. Cell Res. 3, 427–506.

Yadav, S.P., Ibaraki, Y., Dutta Gupta, S., 2010. Estimation of the chlorophyll content of micropropagated potato plants using RGB based image analysis. Plant Cell Tiss. Org. Cult. 100, 183–188.

Yuzhu, H., Xiaomei, W., Shuyao, S., 2011. Nitrogen determination in pepper (*Capsicum frutescens* L.) plants by color image analysis (RGB). Afr. J. Biotechnol. 10, 17737–17741.

Zarco-Tejada, P.J., Berjón, A., López-Lozano, R., Miller, J.R., Martín, P., Cachorro, V., González, M.R., de Frutos, A., 2005. Assessing vineyard condition with hyperspectral indices: leaf and canopy reflectance simulation in a row-structured discontinuous canopy. Remote Sens. Environ. 99, 271–287.

Zude, M., Herold, B., Roger, J.M., Bellon-Maurel, V., Landahl, S., 2006. Non-destructive tests on the prediction of apple fruit flesh firmness and soluble solids content on tree and in shelf life. J. Food Eng. 77, 254–260.